KATHOLIEKE UNIVERSITEIT LEUVEN

thermo research group

New directions in phase-field modeling of microstructure evolution in polycrystalline and multi-component alloys

Nele Moelans

Liesbeth Vanherpe, Jeroen Heulens, Bert Rodiers

K.U. Leuven, Belgium

KATHOLIEKE UNIVERSITEIT LEUVEN

‘Quantitative’ phase-field models

- Properties bulk and interfaces are reproduced accurately in the simulations
  - Effect model description and parameters
  - Numerical issues

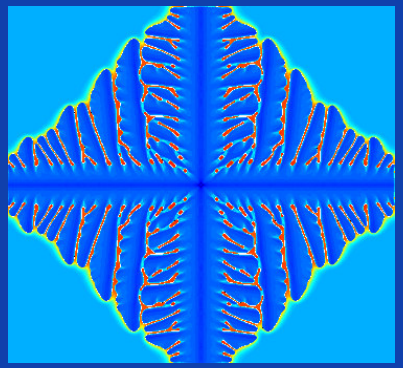

- Insights in the evolution of complex morphologies and grain assemblies
  - Effect of individual bulk and interface properties

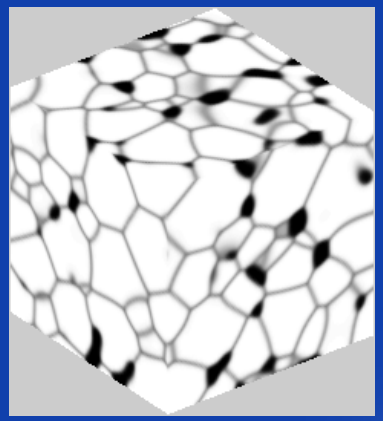

- Predictive ?
  - Depends on availability and accuracy of input data
    - Requires composition and orientation dependence

KATHOLIEKE UNIVERSITEIT LEUVEN

General framework and goal

Experiments, atomistic simulations and thermodynamic models

Crystal structure, phase diagram, interfacial properties (energy, mobility, anisotropy), diffusion properties, …

↓

Phase-field simulations

Microstructure evolution at the mesoscale

↓

Quantitative characterization

Average grain size, grain size distribution, volume fractions, texture,…
Basis for statistical and mean field theories

KATHOLIEKE UNIVERSITEIT LEUVEN

thermo research group

Some aspects of model formulation

- 2-phase systems (single phase-field)
- Multi-grain/phase systems (multiple phase-field)

2-phase systems

- **Field variables:** $\phi(\vec{r},t)$ $\quad c_k(\vec{r},t)$

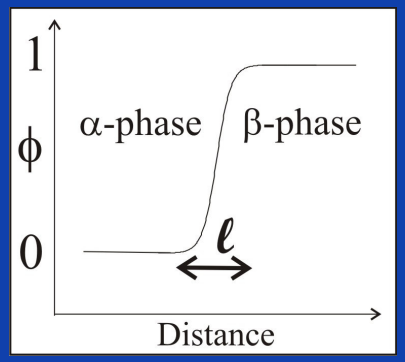

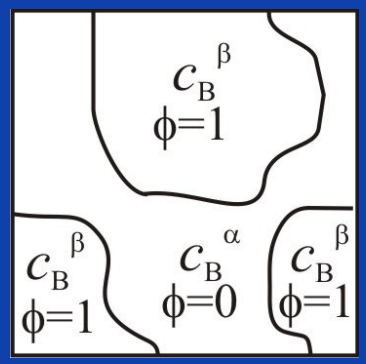

- ***Phase α: ϕ = 0***
- ***Phase β: ϕ = 1***
- ***Composition: c_B***

Double well function

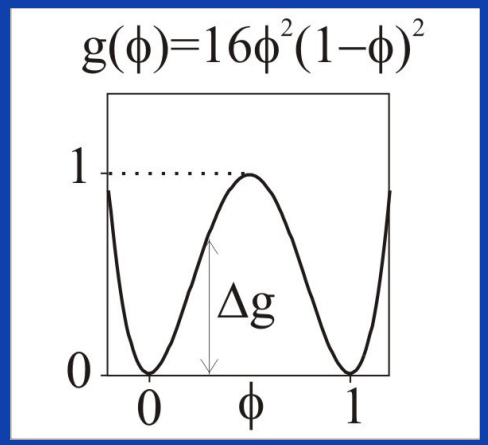

- **Free energy**

$$F = \int_V \left[f_{chem}(c,\phi) + \underbrace{Wg(\phi) + \frac{\varepsilon^2}{2}|\nabla\phi|^2}_{\text{Interfacial energy}} \right] d\vec{r}$$

- **Bulk energy**

$$f_{chem} = h(\phi) f^\beta(c,T) + \left[1 - h(\phi)\right] f^\alpha(c,T)$$

Interpolation function

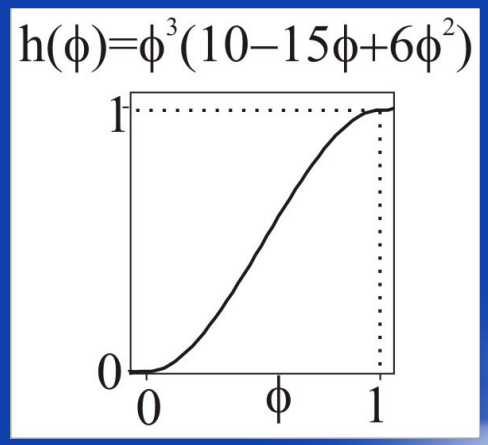

Decoupling bulk and interfacial energy

- **Interface treated as mixture of 2 phases**
  - **c-field for each phase** $c \rightarrow c^{\alpha}, c^{\beta}$
  - **Equal interdiffusion potential + conservation**

$$\begin{cases} \dfrac{\partial f^{\beta}(c^{\beta})}{\partial c^{\beta}} = \dfrac{\partial f^{\alpha}(c^{\alpha})}{\partial c^{\alpha}} = \tilde{\mu} \\ c = h(\phi)c^{\beta} + \left[1 - h(\phi)\right]c^{\alpha} \end{cases}$$

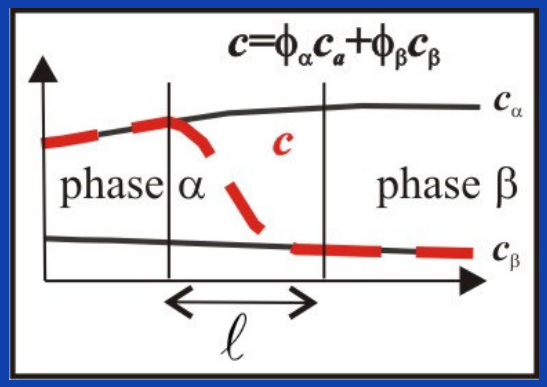

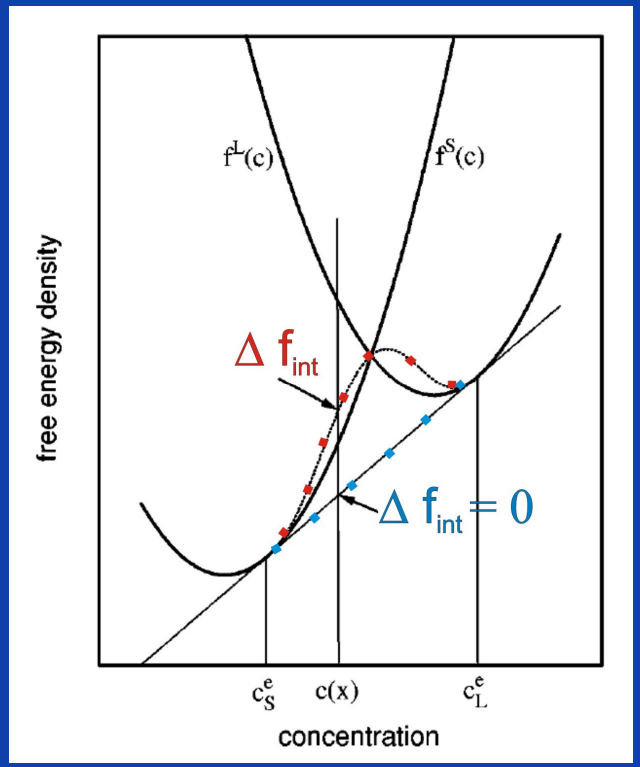

Kim et al., PRE, 6 (1999) p 7186; Tiaden et al., Physica D, 115 (1998) p73

- **Bulk energy**

$$\Rightarrow f_{chem} = h(\phi)\, f^{\beta}(c^{\beta}) + \left[1 - h(\phi)\right] f^{\alpha}(c^{\alpha})$$

Decoupling bulk and interfacial kinetics

- **Kinetic equations (Linear non-equilibrium thermodynamics)**
  - **Allen-Cahn** $$\frac{\partial \varphi}{\partial t} = -M_{\varphi} \frac{\partial F}{\partial \varphi}$$
  - **Diffusion** $$\frac{\partial c_k}{\partial t} = \nabla \cdot \sum_{l}^{C-1} \left[h(\phi) M_{kl}^{\beta} + [1 - h(\phi)] M_{kl}^{\alpha} \right] \nabla \tilde{\mu}_l$$
- **Jump in chemical potential accross interface**

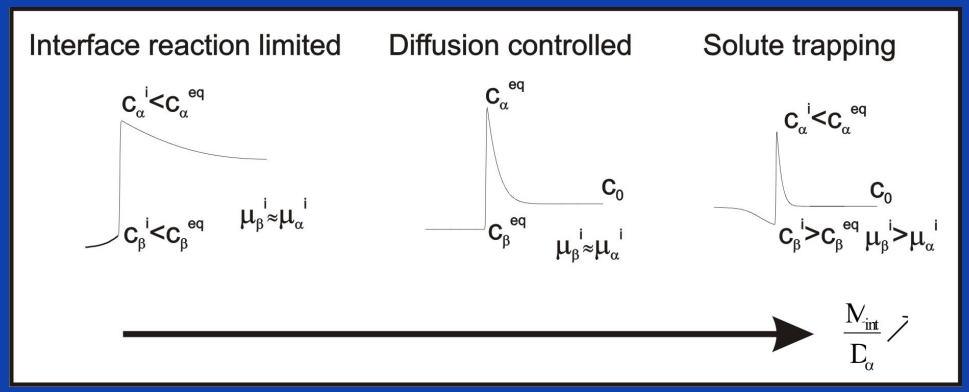

$$\frac{\partial c_k}{\partial t} = \nabla \cdot [1 - h(\phi)] \sum_{l=1}^{C-1} M_{kl}^{L} \nabla \tilde{\mu}_l + \underbrace{\nabla \cdot \alpha_i \frac{\partial \phi}{|\partial t|} \frac{\nabla \phi}{|\nabla \phi|}}_{\text{Non-variational anti-trapping current}}$$

Solute trapping effect

$$\Delta \mu_i \propto \ell$$

$$\Delta \mu_i \propto v_n$$

- ***Dilute, D_S=0**: A.Karma, PRL, 87, 115701 (2001); B. Echebarria et al., PRE, 70, 061604 (2004)*
- ***Multi-comp, D_S=0**: S.G. Kim, Acta Mater. 55, p4391 (2007)*

Multi-grain and multi-phase structures

- **Single phase-field models -> Multiple phase-field models**

$$\eta \rightarrow \{\eta_1, \eta_2, \eta_3, \ldots, \eta_p\}$$

$$(\eta_1, \eta_2, \ldots, \eta_i, \ldots, \eta_p) = (0, 0, \ldots, 1, \ldots, 0)$$

  - **Model extension**

$$F(\eta_1, \eta_2, \eta_3, \ldots, |\nabla \eta_1|^2, |\nabla \eta_2|^2, \ldots)$$

    - **Different types of interfaces**
    - **Triple and higher order junctions**

  - **Numerically**
    - **Same accuracy for all interfaces and phases**
    - **All interfaces within range of validity of the thin interface asymptotics**

$$\rightarrow \ell_{num} = cte$$

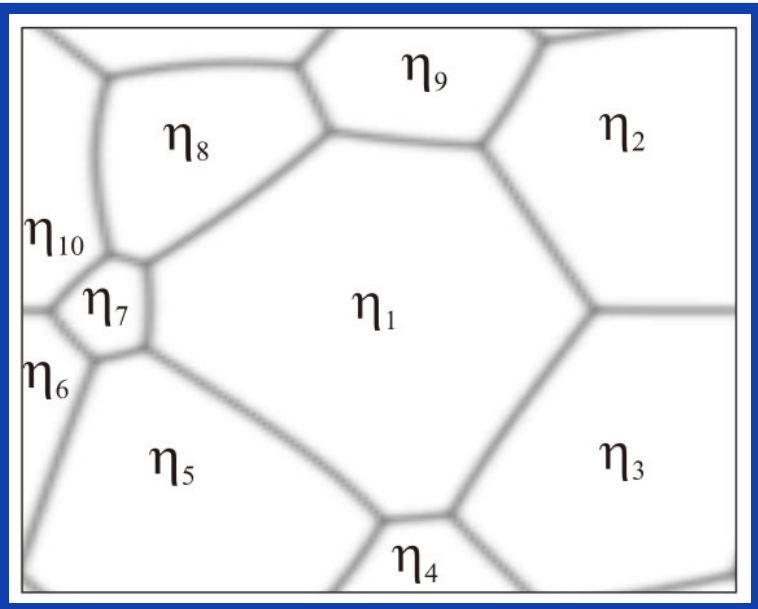

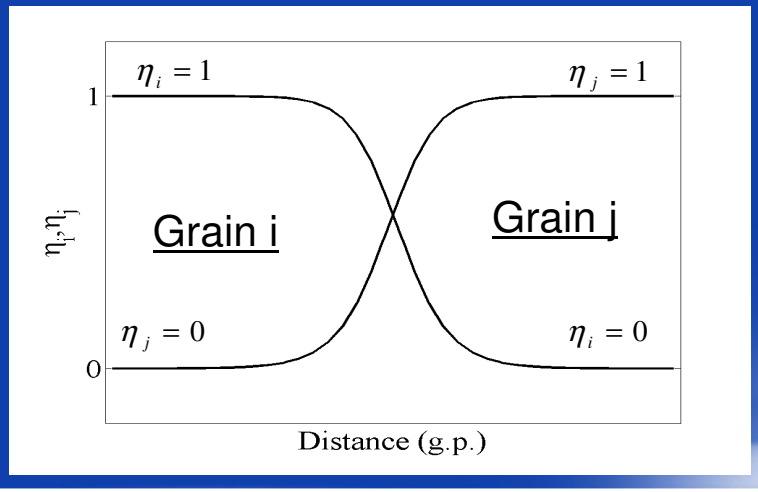

Multi-grain and multi-phase models: major difficulties

- **Third-phase contributions**
  - $\sigma_{12} = \sigma_{13} = 7/10\ \sigma_{12}$

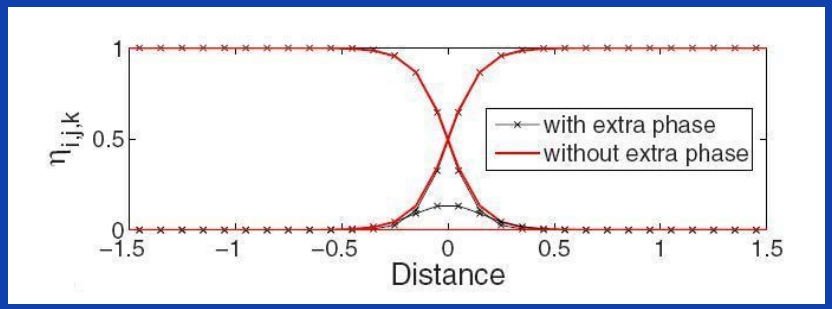

  - → Careful choice of multi-well function and gradient contribution

η_3

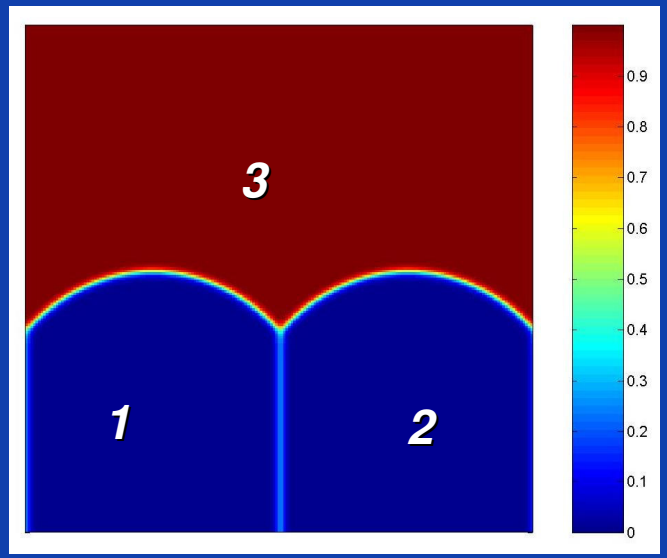

- **Interpolation function**
  - Zero-slope at equilibrium values of the phase fields
  - Thermodynamic consistency

$$f_{chem} = \sum_{i=1}^{p} h_i(\eta_1, \eta_2, \ldots) f^i(c,T) \quad \Rightarrow \sum_{i=1}^{p} h_i(\eta_1, \eta_2, \ldots) = 1$$

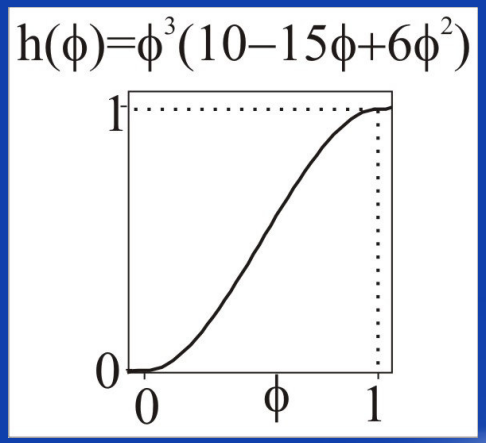

KATHOLIEKE UNIVERSITEIT LEUVEN

Anisotropic grain growth model

- **Phase fields** $\eta_1, \eta_2, \ldots, \eta_i(\vec{r}, t), \ldots, \eta_p$
  - **With grain i**

$$(\eta_1, \eta_2, \ldots, \eta_i, \ldots, \eta_p) = (0, 0, \ldots, 1, \ldots, 0)$$

- **Free energy**

$$F_{interf} = \int_V m\left(\sum_{i=1}^{p}\left(\frac{\eta_i^4}{4} - \frac{\eta_i^2}{2}\right) + \sum_{i=1}^{p}\sum_{j<i}^{p}\gamma_{i,j}\eta_i^2\eta_j^2 + \frac{1}{4}\right) + \frac{\kappa(\eta)}{2}\sum_{i=1}^{p}(\nabla\eta_i)^2 dV$$

$$\kappa(\eta) = \sum_{i=1}^{p}\sum_{j<i}^{p}\kappa_{i,j}\eta_i^2\eta_j^2 \Big/ \sum_{i=1}^{p}\sum_{j<i}^{p}\eta_i^2\eta_j^2$$

  - **For each grain boundary** $\eta_i^2\eta_j^2 \neq 0 \Rightarrow \kappa(\eta) = \kappa_{i,j}$

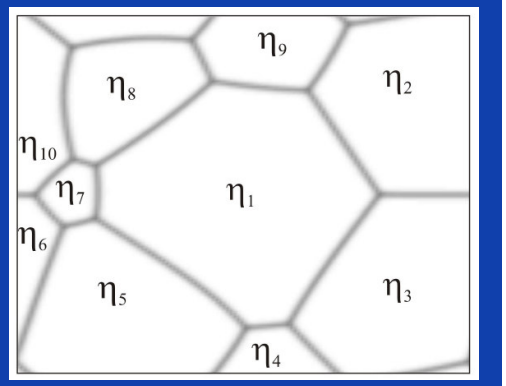

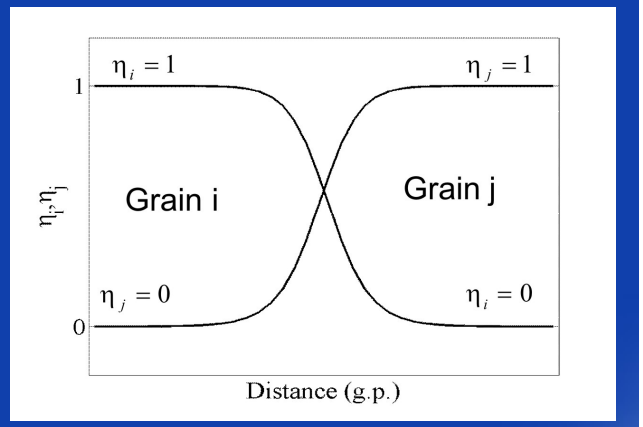

- **Inclination dependence**

$$\gamma_{i,j}(\psi_{i,j}), \kappa_{i,j}(\psi_{i,j}), L_{i,j}(\psi_{i,j}), \qquad \psi_{i,j} = \frac{\nabla\eta_i - \nabla\eta_j}{|\nabla\eta_i - \nabla\eta_j|}$$

L.-Q. Chen and W. Yang, PRB, 50 (1994) p15752

A. Kazaryan et al., PRB, 61 (2000) p14275

Non-variational approach – equal interface width

- **Ginzburg-Landau type equations**

$$\frac{\partial \eta_i(\vec{r},t)}{\partial t} = -L(\eta)\left[m\left(\eta_i^3 - \eta_i + 2\eta_i \sum_{j\neq i} \gamma_{i,j}\eta_j^2 \right) - \kappa(\eta)\nabla^2\eta_i \right]$$

  - **Non-variational with respect to η-dependence of κ**
  - **Similar to Monte Carlo Potts approach**

- **Definition 'grain boundary width'**

$$l_{num} = \frac{1}{\left|\frac{d\eta_i}{dx}\right|_{\max}} = \frac{1}{\left|\frac{d\eta_j}{dx}\right|_{\max}}$$

→High controllability of numerical accuracy ($l_{num}/R < 5$)

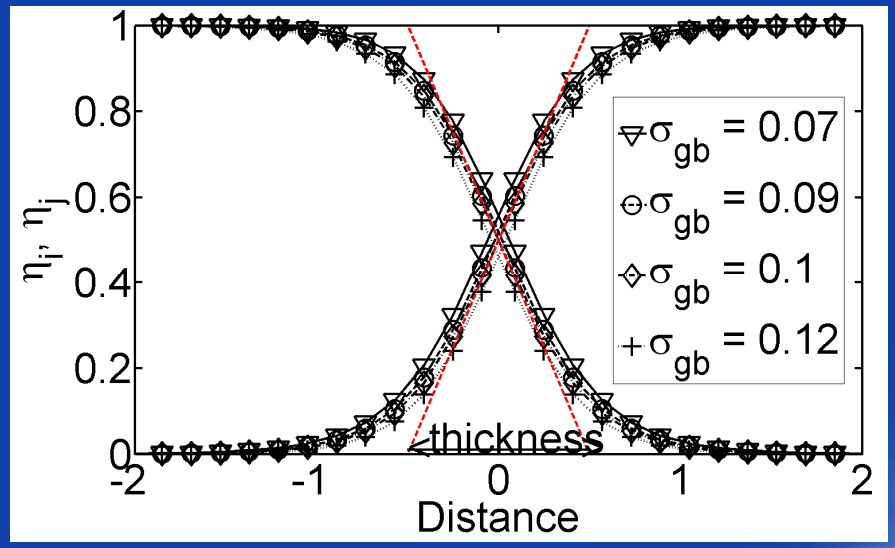

KATHOLIEKE UNIVERSITEIT LEUVEN

Grain boundary properties

- **Grain boundary energy**

$$\gamma_{gb,\theta_{i,j}} = g(\gamma_{i,j})\sqrt{m\kappa_{i,j}}$$

- **Grain boundary mobility**

$$\mu_{gb,\theta_{i,j}} = L_{i,j}\sqrt{\frac{\kappa_{i,j}}{m(g(\gamma_{i,j}))^2}}$$

- **Grain boundary width**

$$l = \frac{4}{3}\sqrt{\frac{\kappa_{i,j}}{m(g(\gamma_{i,j}))^2}}$$

- **Iterative algorithm**

$$\ell_{gb},[\gamma_{gb,\theta}],[\mu_{gb,\theta}] \rightarrow m,[\kappa_{i,j}],[\gamma_{i,j}],[L_{i,j}]$$

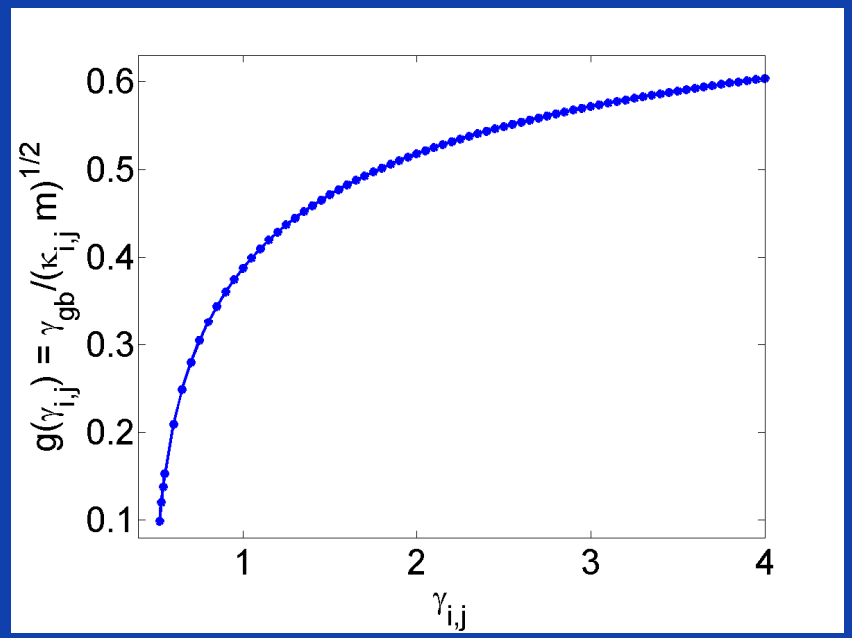

$g(\gamma_{i,j})$ calculated numerically

N. Moelans, B. Blanpain, P. Wollants, PRL, 101, 0025502 (2008); PRB, 78, 024113 (2008)

KATHOLIEKE UNIVERSITEIT LEUVEN

Numerical validation

- **Shrinking grain:**

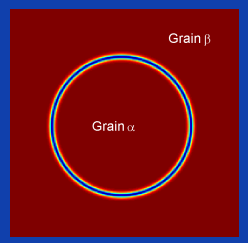

$$\frac{dA_\alpha}{dt} = -2\pi\mu_{\alpha\beta}\sigma_{\alpha\beta}$$

- **Triple junction angles:**

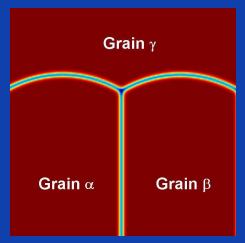

$$\frac{dA_\alpha}{dt} = -\mu_{\alpha\gamma}\sigma_{\alpha\beta}$$

$\sigma_{\alpha\gamma} = \sigma_{\beta\gamma}, \mu_{\alpha\gamma} = \mu_{\beta\gamma}$

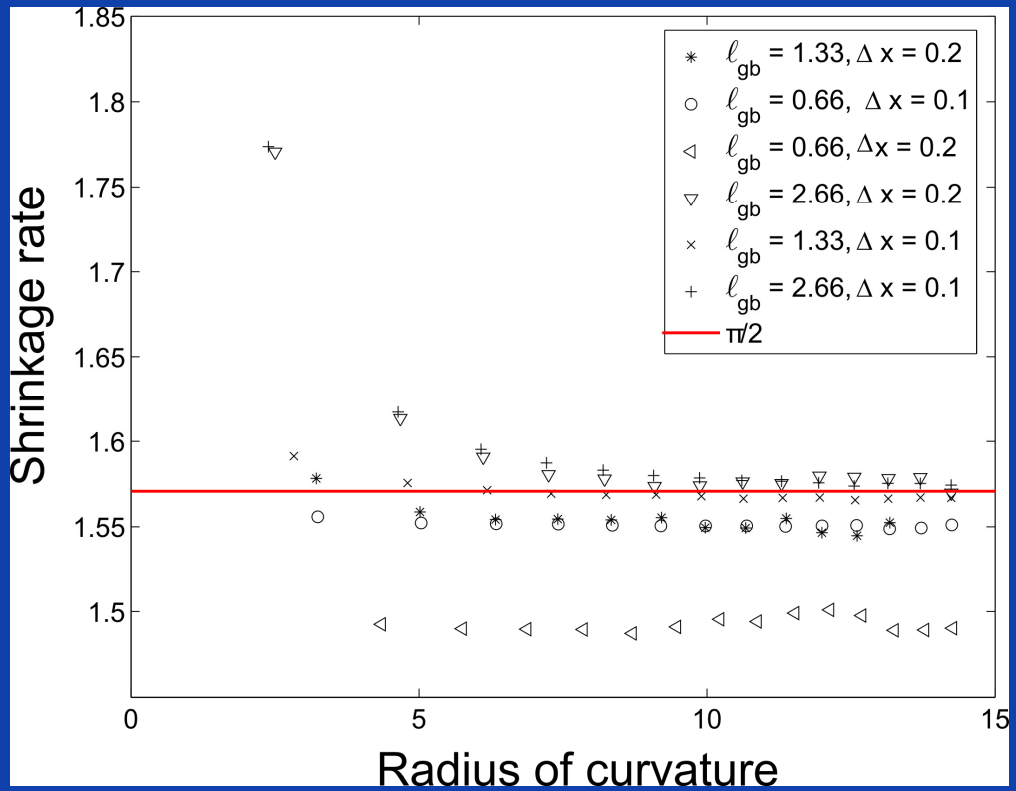

- **Observations**
  - **Accuracy controlled by** $\ell_{num} / \Delta x$
  - **Diffuse interface effects for** $\ell_{num} / R > 5$
  - **Angles outside [100°-140°] require larger** $\ell_{num} / \Delta x$ **for same accuracy**

Variational approach – interface width varies with interface energy

- **Anisotropy only through** $\gamma_{i,j}$, κ=cte
  - **Energy**

$$F = \int_V \left[m \left(\sum_{i=1}^{p} \left(\frac{\eta_i^4}{4} - \frac{\eta_i^2}{2} \right) + \sum_{i=1}^{p} \sum_{j<i}^{p} \gamma_{i,j} \eta_i^2 \eta_j^2 + \frac{1}{4} \right) + \frac{\kappa}{2} \sum_{i=1}^{p} (\vec{\nabla} \eta_i)^2 \right] dV$$

  - **Kinetic equations**

$$\frac{\partial \eta_i(\vec{r},t)}{\partial t} = -L(\eta) \left[m \left(\eta_i^3 - \eta_i + 2\eta_i \sum_{j \neq i} \gamma_{i,j} \eta_j^2 \right) - \kappa \nabla^2 \eta_i \right]$$

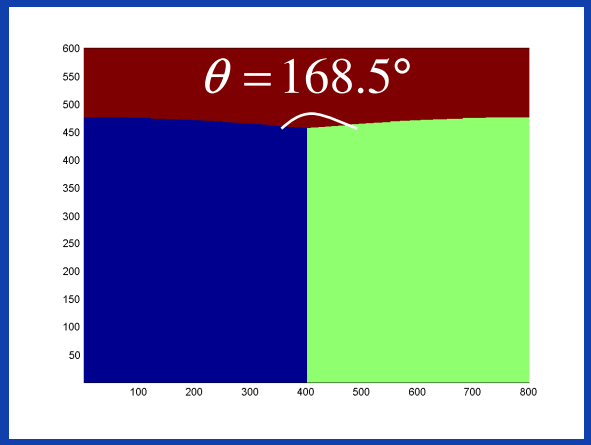

$\sigma_{13} = \sigma_{23} = 5\sigma_{12}$

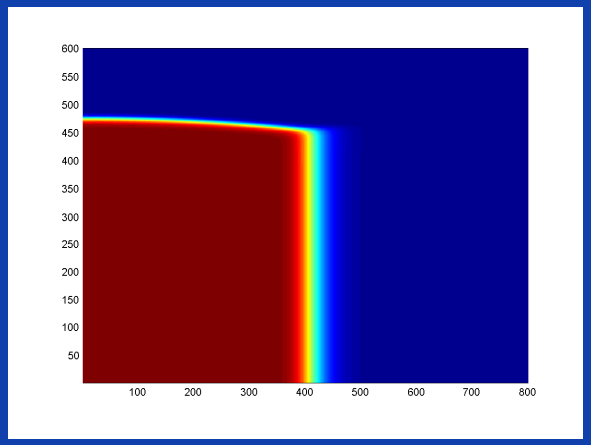

η_1

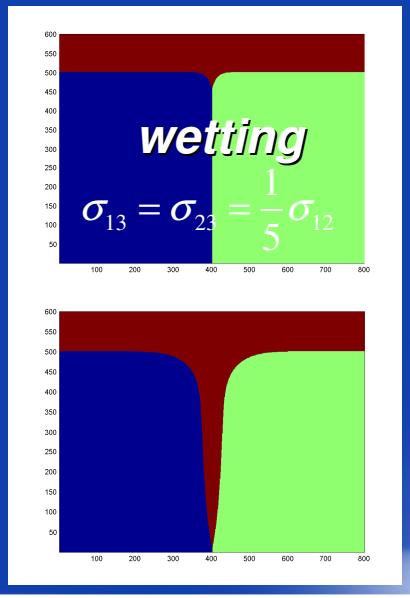

Rotation invariance of the model

- **Mathematically, the model equations are invariant to rotation, but …**
- **the order parameters represent <u>orientations</u> in a fixed reference frame.**

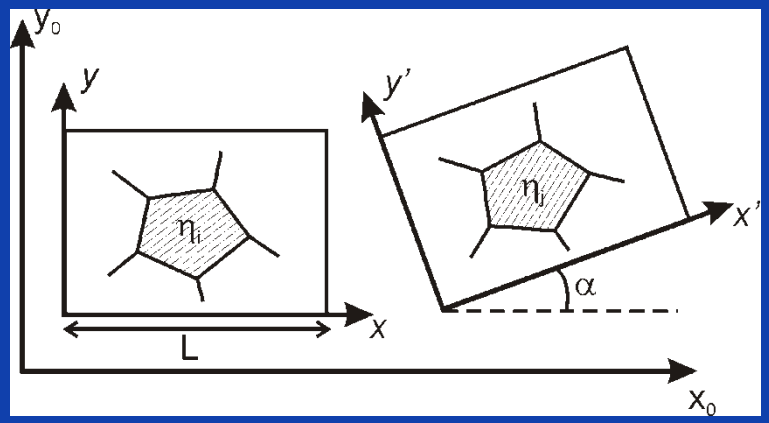

grid spacing Δh

physical width of domain L

rotational symmetry n

- **The precision of α depends on the numerical setup,**

$$\Delta\alpha \approx \frac{1}{\cos\alpha}\frac{\Delta h}{L}$$

- **For the model to be rotational invariant in practice, lower limit of amount of order parameters *p*:**

$$p > \frac{\sqrt{2}\pi L}{n\Delta h}$$

J. Heulens and N. Moelans, Scripta Mat. (2010)

Extension to multi-component multi-phase alloys

- **Phase field variables:**
  - **Grains** $\eta_{\alpha 1}, \eta_{\alpha 2}, \ldots, \eta_{\alpha i}(\vec{r}, t), \ldots,$ $\eta_{\beta 1}, \eta_{\beta 2}, \ldots \eta_p$
  - **Composition** $c_A, c_B(\vec{r}, t), \ldots, c_{C-1}$

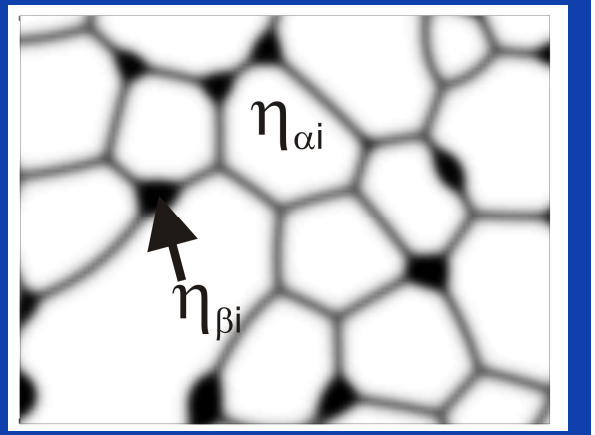

- **Bulk energy:** $f_{bulk}(c_k, \eta_{\rho i}) = \sum_{\rho} \phi_\rho f^\rho(c_k^\rho)$
  - **with**

$$\begin{cases} \dfrac{\partial f^\beta(c_k^\beta)}{\partial c_k^\beta} = \dfrac{\partial f^\alpha(c_k^\alpha)}{\partial c_k^\alpha} = \ldots = \tilde{\mu}_k \\ x_k = \sum_\rho \phi_\rho x_k^\rho \end{cases}$$

and $$\phi_\rho = \frac{\sum_i \eta_{\rho i}^2}{\sum_{\pi=\alpha,\beta,\ldots} \sum_i \eta_{\pi i}^2}$$

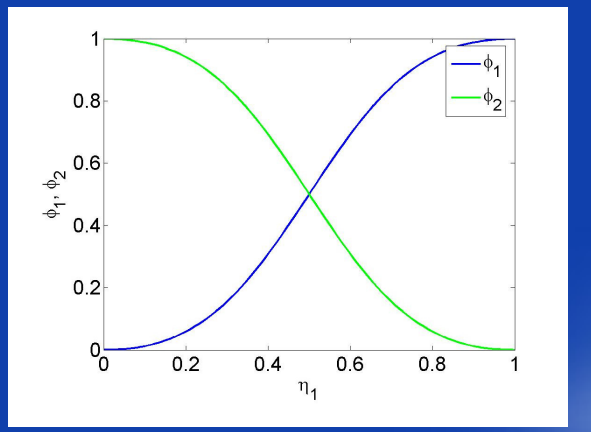

Extension to multi-component multi-phase alloys

- **Bulk and interface diffusion:**

$$\frac{\partial x_k}{\partial t} = \nabla \cdot \left[\left(\sum_{\rho} \phi_\rho M_k^\rho + \sum_{\rho, i \neq \sigma, j} \eta_{\rho,i}^2 \eta_{\sigma,j}^2 \right) \nabla \mu_k \right]$$

With

$$M_k^\rho = \frac{D_k^\rho}{\frac{\partial^2 f_m^\rho}{\partial x_k^2}}$$

and

$$M_{interf} = 3 \left(\frac{D_{interf}}{\partial^2 f^m / \partial x_k^2} \right) \left(\frac{\delta_{gb}}{\delta_{num}} \right)$$

- **Interface movement:**

$$\frac{\partial \eta_{i\rho}}{\partial t} = -L \frac{\delta F(\eta_{i\rho}, x_k)}{\delta \eta_{i\rho}}$$

  - **Between phase α and β**

$$\frac{\partial \eta_{\alpha i}}{\partial t} = -L \left(g_{\text{int}}(\eta, \nabla \eta) + \frac{2 \eta_{\alpha i} \eta_{\beta j}^2}{\left(\eta_\alpha^2 + \eta_\beta^2\right)^2} \left(f^\alpha(c^\alpha) - f^\beta(c^\beta) - (c^\alpha - c^\beta)\mu \right) \right)$$

Curvature driven *Bulk energy driven*

Numerical validation for multi-component multi-phase model

- *Triple junction*

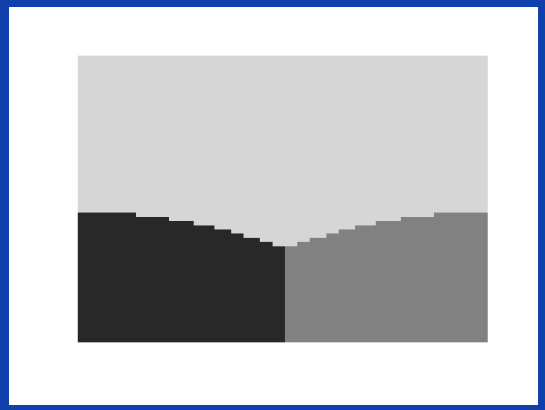

- *Growing sphere*

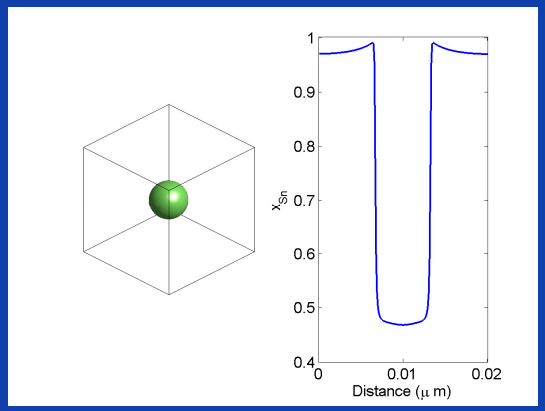

- *Intermediate phase*

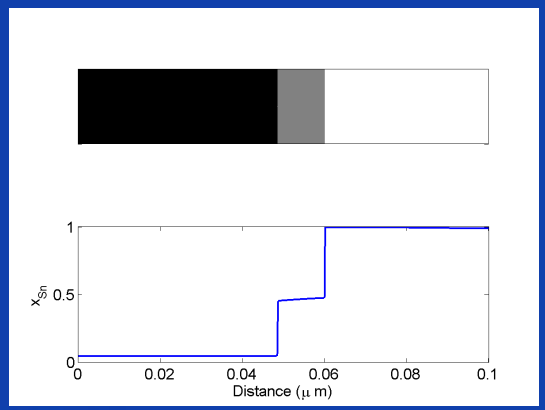

- *Coarsening*

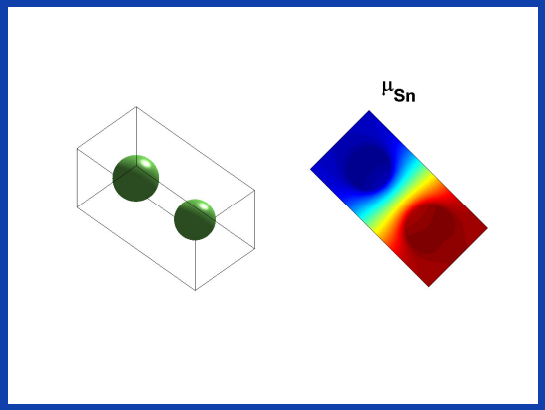

- **Processes for which v(t) ↘**
- **Conclusions for grain growth model remain**
  - **Accuracy controlled by $\ell_{num} / \Delta x$**
  - **Diffuse interface effects for $\ell_{num} / R > 5$**
  - **Angles outside [100°-140°] require larger resolution $\ell_{num} / \Delta x$ for same accuracy**

Bounding Box Implementation

- **Basic elements**
  - **A grain is set of connected grid points r where |eta_i(r)| > epsilon**
  - **For each grain, the corresponding bounding box is the smallest cuboid containing the grain**

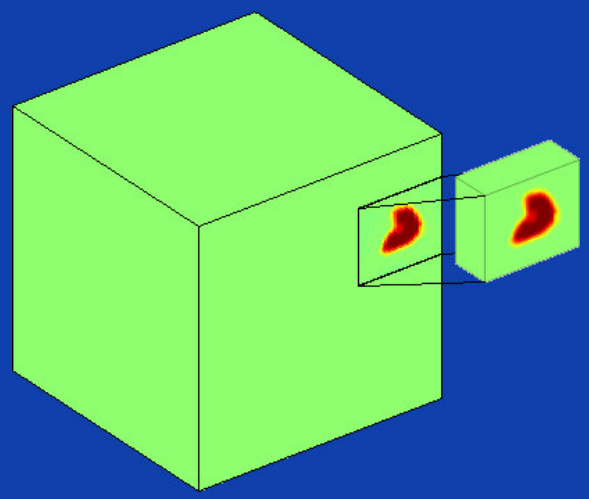

Algorithm

Solve the equations only locally, inside bounding boxes

Only values inside boxes are kept in memory

Boxes grow or shrink with grain

Object Oriented C++ implementation

- *In collaboration with* L. Vanherpe and S. Vandewalle, K.U. Leuven (*Vanherpe et al., PRE, 76, n° 056702 (2007))*

KATHOLIEKE UNIVERSITEIT LEUVEN

thermo research group

Application examples

- **Grain growth in anisotropic systems with a fiber texture**

- *In collaboration with* F. Spaepen, Harvard University

Grain growth in columnar films with fiber texture

- Grain boundary energy:
  - Fourfold symmetry
  - Extra cusp at θ = 37.5°
  - Read-shockley

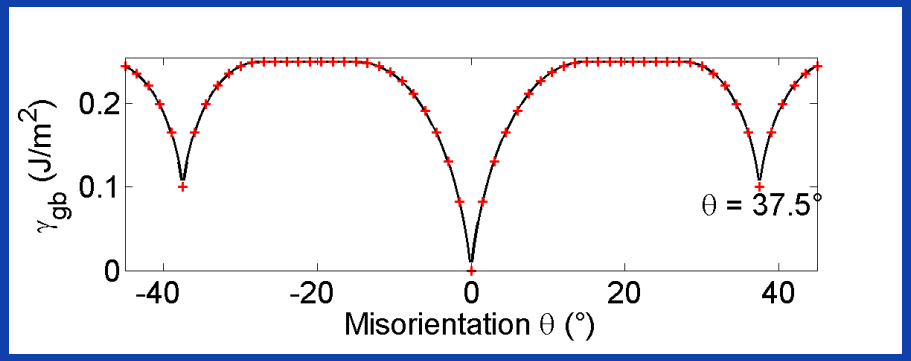

- Discrete orientations

$$\eta_1, \eta_2, \ldots, \eta_i(\vec{r}, t), \ldots, \eta_{60} \Rightarrow \Delta\theta = 1.5°$$

- Constant mobility
- Initially random grain orientation and grain boundary type distributions

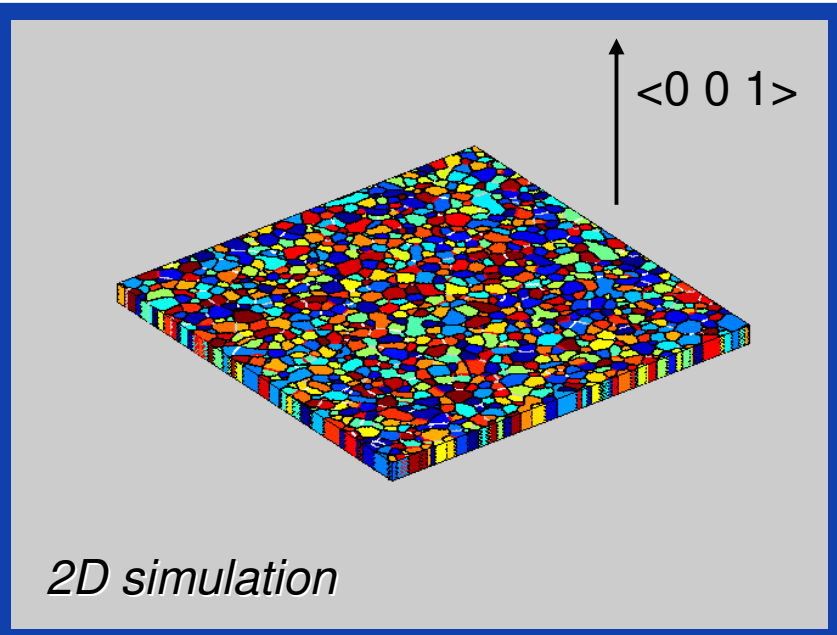

White: $\theta = 1.5$
Gray: $\theta = 3$
Red: $\theta = 37{,}5$
Black: $\theta > 3$, $\theta \neq 37.5$

KATHOLIEKE UNIVERSITEIT LEUVEN

Simulations: 1 high-angle energy cusp

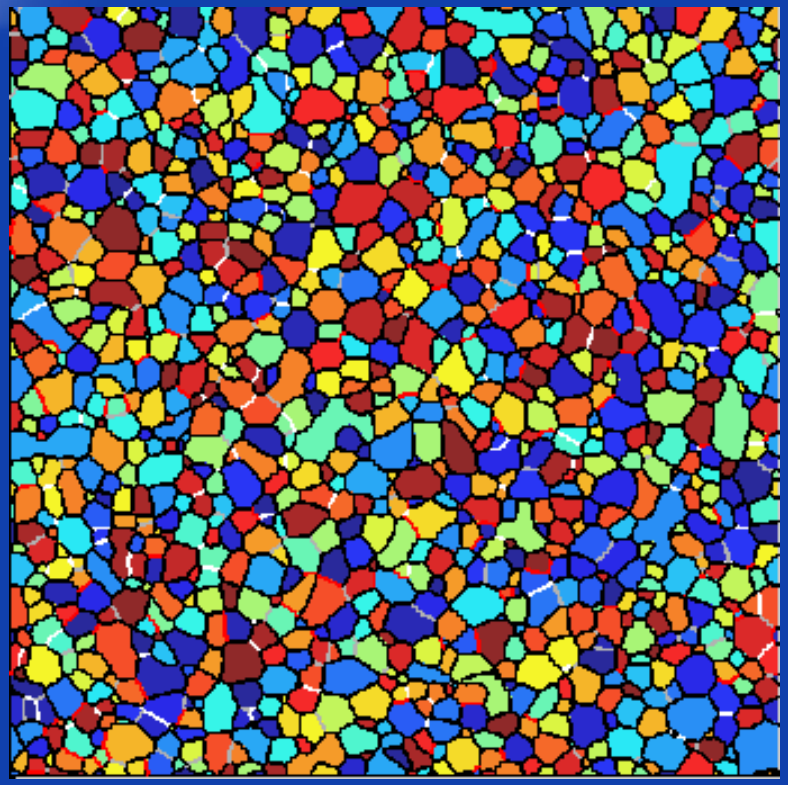

- High-angle grain boundaries form independent network
- Low-angle grain boundaries follow movement of high-angle grain boundaries → elongate
- No stable quadruple junctions

White: $\theta = 1.5$
Gray: $\theta = 3$
Black: $\theta > 3$, $\theta \neq 37.5$
Red: $\theta = 37{,}5$

Misorientation distribution function (MDF)

- **Area weigthed MDF**

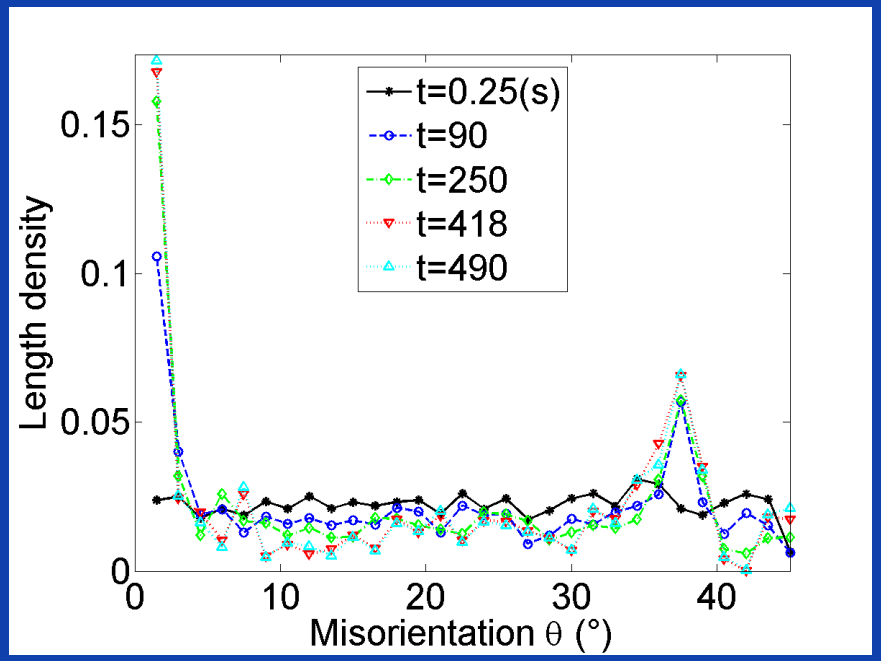

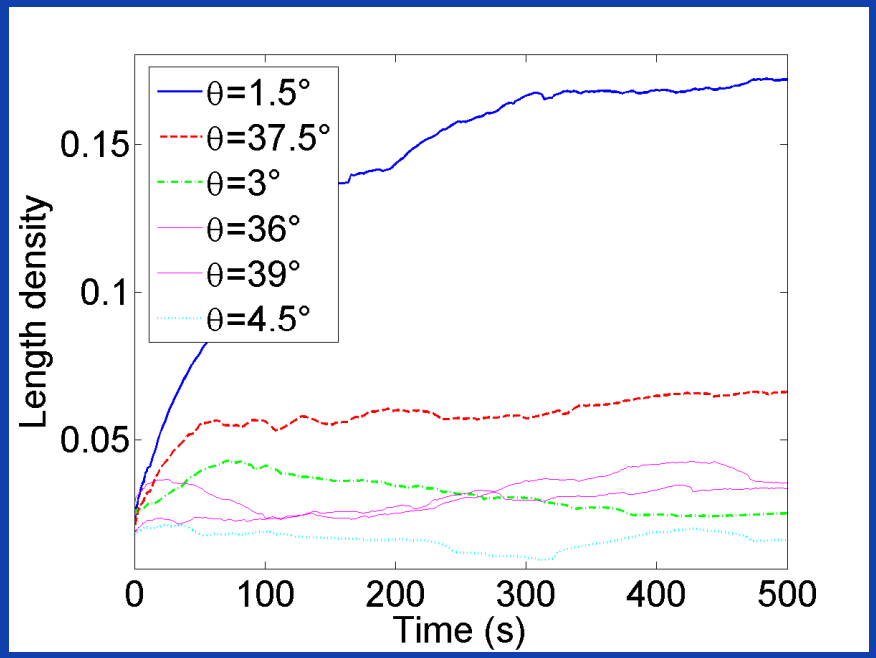

Read-Shockley + cusp at θ = 37.5°

- **Reaches a stead-state**
- **Low energy boundaries lengthen + their number increases**

KATHOLIEKE UNIVERSITEIT LEUVEN

Grain growth kinetics

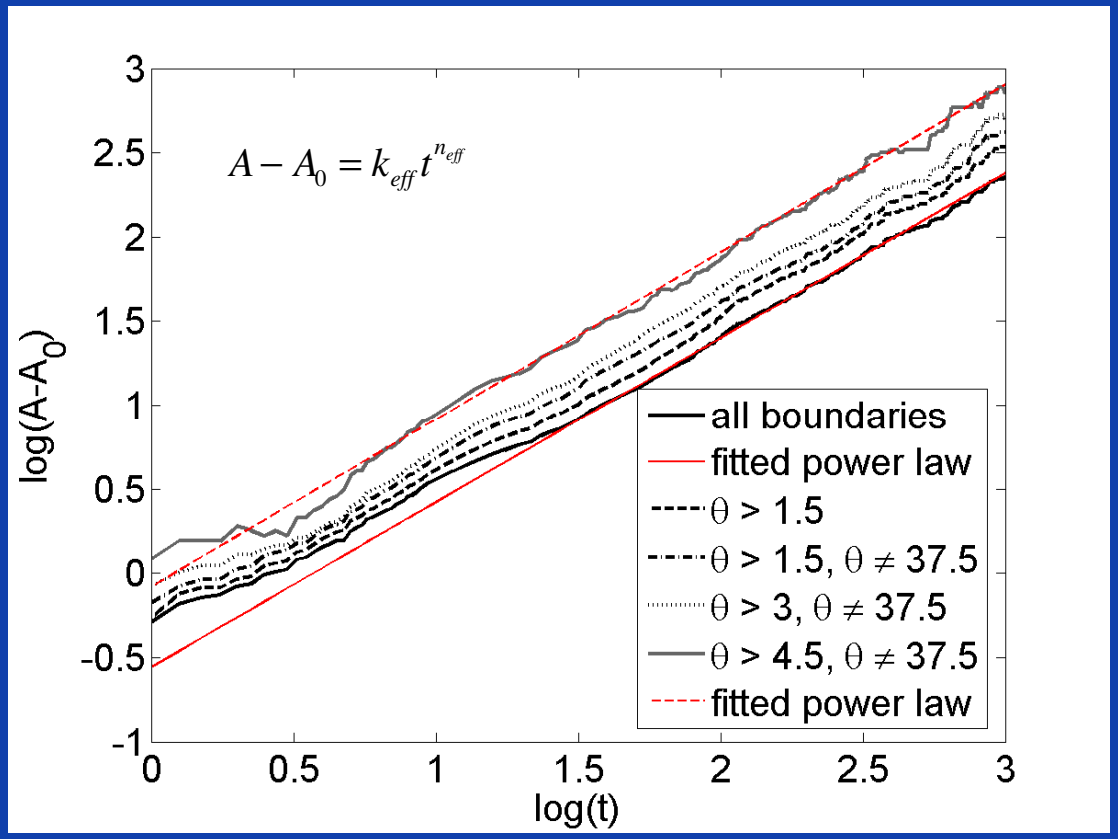

Read-Shockley (θ_m=15°) + cusp at θ=37.5°

- **Grain growth exponent**
  - **PFM: steady-state growth with**
    $n \approx 1$
  - **Previous findings:**
    $n = 0.6 \ldots 1$
  - **Mean field analysis:**

$$n_{eff} = \frac{kt}{A_h(0) + kt} \rightarrow 1, t \rightarrow \infty$$

$$k_{eff} = \frac{dA_{eff}}{dt} = \frac{k}{1 + N'/N}$$

N. Moelans, F. Spaepen, P. Wollants, Phil. Mag., 90 p 501-523 (2010)

KATHOLIEKE UNIVERSITEIT LEUVEN

thermo research group

Application examples

- **Coarsening of Al_6Mn precipitates located on a recrystallization front in Al-Mn alloys**

In collaboration with A. Miroux, E. Anselmino, S. van der Zwaag, T. U. Delft

KATHOLIEKE UNIVERSITEIT LEUVEN

Jerky motion during recrystallization in Al-Mn alloy

- **In-situ EBSD observation of recrystallization in AA3103 at 400 ℃**
  - **CamScan X500 Crystal Probe FEGSEM**
- **Jerky grain boundary motion**
  - **Stopping time: 15-25 s**
  - **Pinning by second-phase precipitates**
    - **$Al_6(Fe,Mn)$, α-$Al_{12}(Fe,Mn)_3Si$**
- **Added to phase field model**
  - **Grain boundary diffusion**
  - **Driving force for recrystallization**

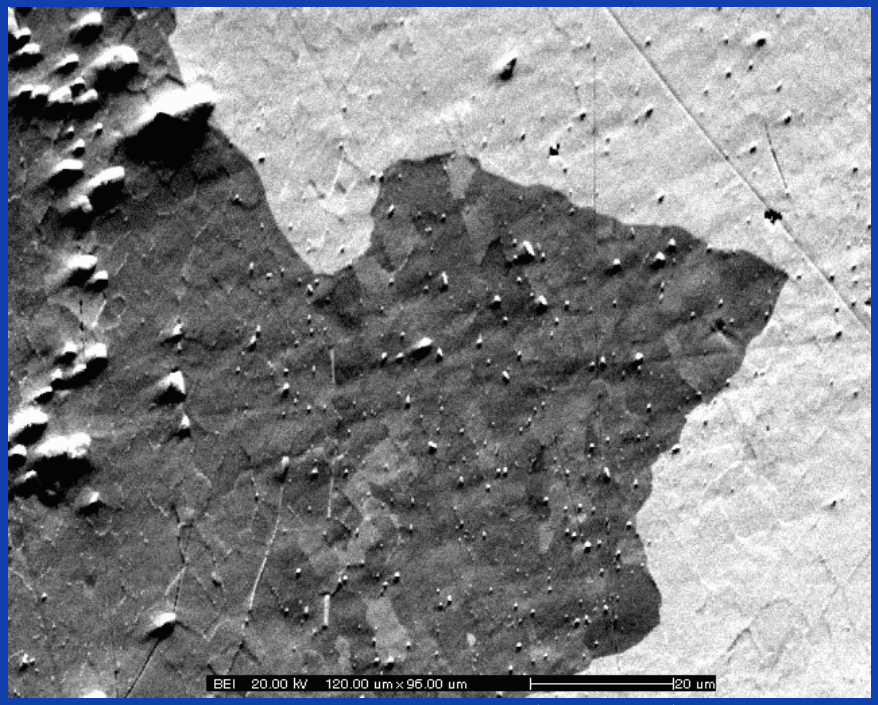

20μm

Phase field model

- **Multiple order parameter representation:** $\eta_{m,1}(\vec{r},t),\eta_{m,2}(\vec{r},t),\ldots,\eta_{p,i}(\vec{r},t),\ldots$

$$(\eta_{m,1},\eta_{m,2},\ldots,\eta_{p,i},\ldots)=(1,0,\ldots,0,\ldots),(0,1,\ldots,0,\ldots),\ldots(0,0,\ldots,1,\ldots),\ldots$$

- **Mn composition field:** $x_{Mn}(\vec{r},t)$
- **Homogeneous driving pressure for recrystallization:** m_d
- **Bulk diffusion + Surface diffusion**

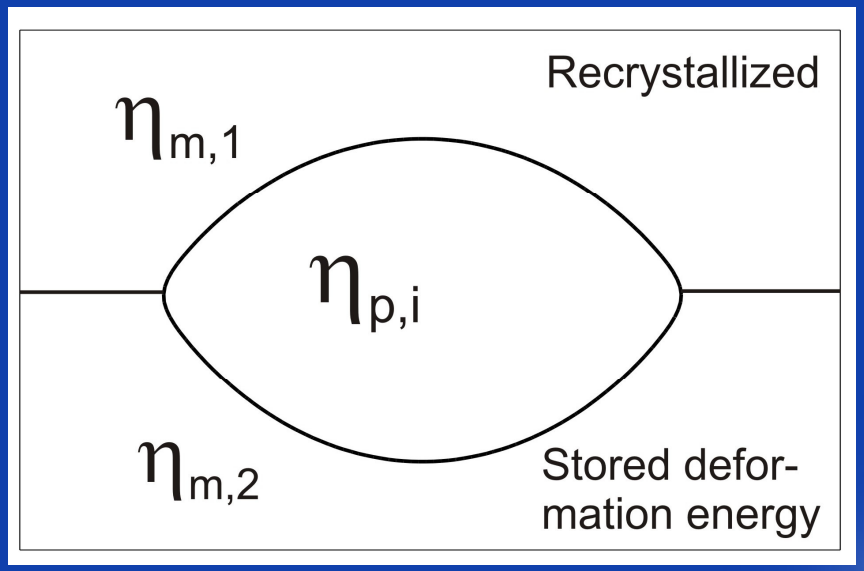

KATHOLIEKE UNIVERSITEIT LEUVEN

Material properties at 723K

Grain boundary energy high angle	γ_h = 0.324 J/m^2
Interfacial energy Al_6Mn precipitates	γ_{pr} = 0.3 J/m^2
Mobility high angle grain boundary At solute content 0.3w% Mn	$M_h = 2.94 \cdot 10^{-11}$ m^{2}s/kg (Miroux et al.,Mater. Sci. Forum,467-470,393(2004))
Equilibrium composition of matrix	$c_{Mn,eq}$ = 0.0524 w% (0.02456 at%) (PhD thesis Lok 2005)
Actual composition of matrix (supersaturated)	c_{Mn} = 0.3 w% (0.1474 at%) (PhD thesis Lok 2005)
Mn diffusion in fcc Al	$D_{0,bulk} = 10^{-2}$ m^2/s, Q_{bulk} = 211 kJ/mol $\rightarrow D_{bulk} = 5.5973 \cdot 10^{-18}$ m^2/s
Pipe diffusion high angle boundaries, precipitate/matrix interface	$D_{0,p} = D_{0,bulk}$, $Q_p = 0.65 Q_{bulk}$ $\rightarrow D_p = 1.2195 \cdot 10^{-12}$ m^2/s
Bulk energy density: $f^\rho = A^\rho (x - x^\rho_0)^2$	$A^m = 6 \cdot 10^{11}$; $x^m_0 = 0.000258$ $A^\rho = 6 \cdot 10^{12}$; $x^\rho_0 = 0.1429$

Precipitate coarsening and unpinning

- $P_D < P_{ZS}$ ($P_D \approx P_{ZS}$)
  - Pinning: P_{ZS}=3.6 MPa
  - Rex: P_D=3.1 MPa

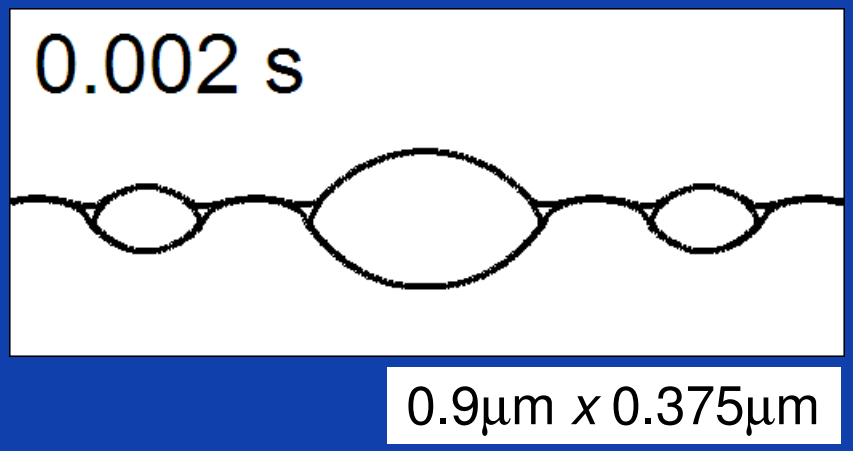

- Unpinning mainly through surface diffusion around precipitates

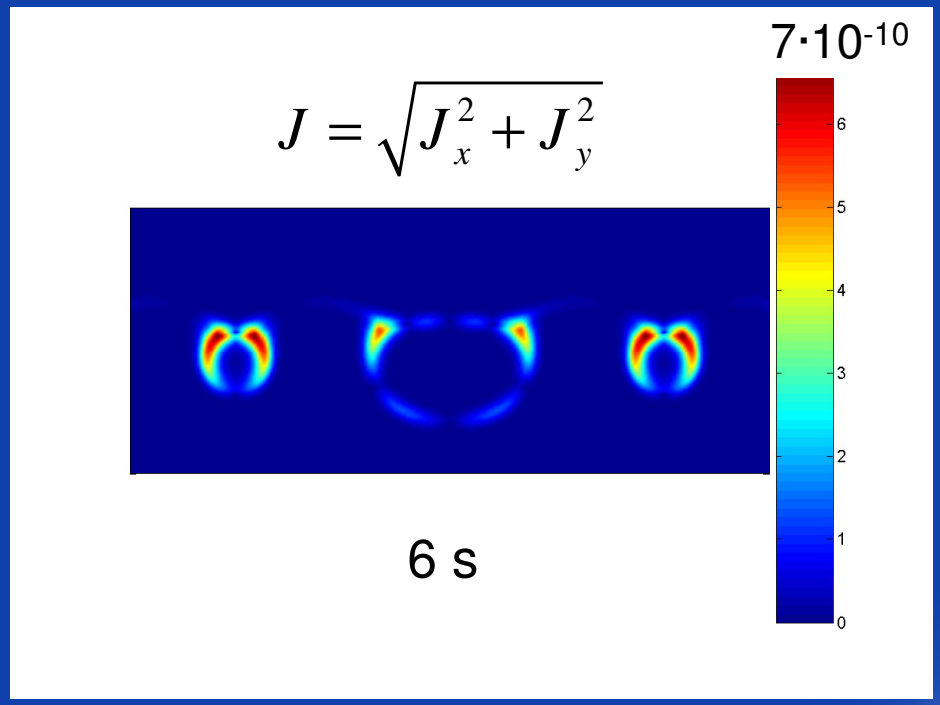

Precipitate coarsening and unpinning

- $P_D <<< P_{ZS}$
  - Pinning: P_{ZS} = 3.6 MPa
  - Rex: P_D = 1.1 MPa

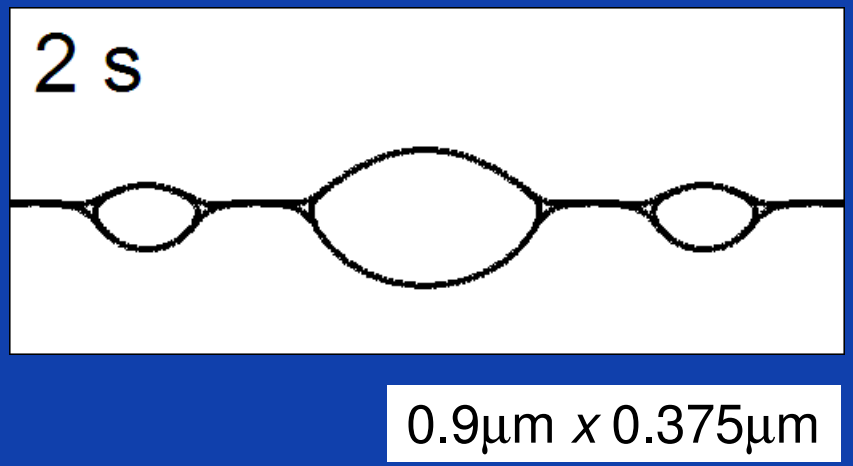

- Unpinning through grain boundary diffusion

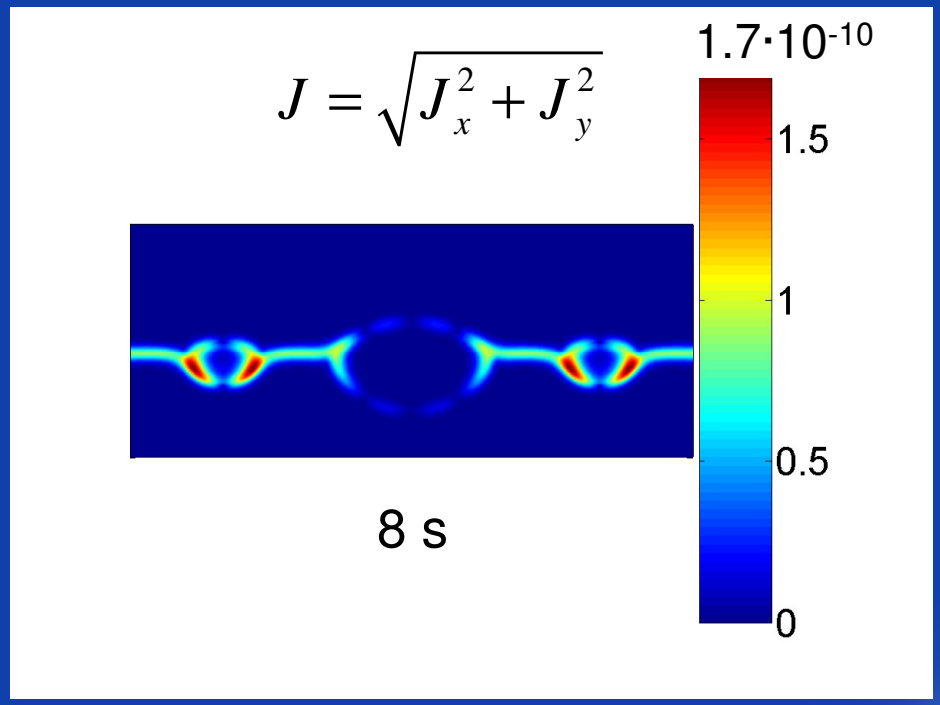

KATHOLIEKE UNIVERSITEIT LEUVEN

thermo research group

Application examples

- **Coarsening and diffusion controlled growth in lead-free solder joints**

Within the framework of COST MP-0602 (Advanced Solder Materials for High Temperature Application), Chairs A. Kroupa and A. Watson

KATHOLIEKE UNIVERSITEIT LEUVEN

Coarsening in Sn(-Ag)-Cu solder joints

- **IMC formation and growth – precipitate growth – Kirkendal voids – stresses – grain boundary diffusion**
  - **CALPHAD description**
  - **Diffusion coefficients, growth coefficient for IMC-layers**

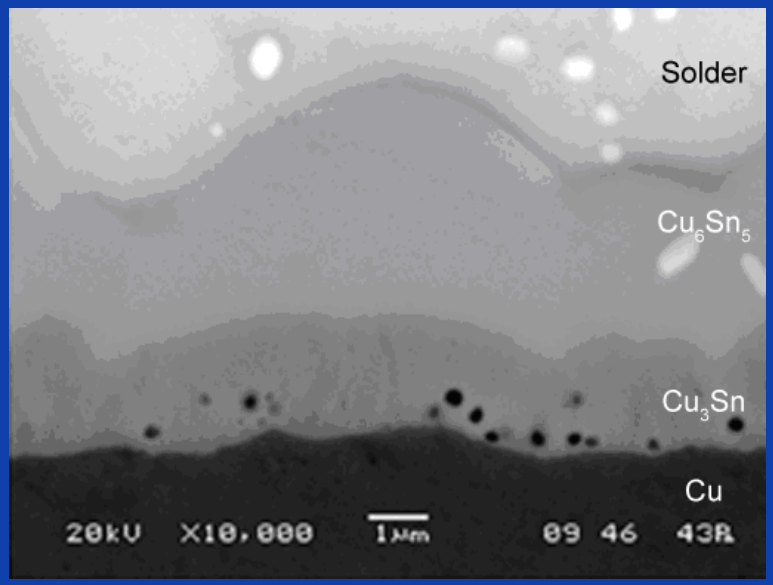

SEM-image of Sn – 3.8Ag–0.7 Cu alloy after annealing for 200h at 150°C (Peng 2007)

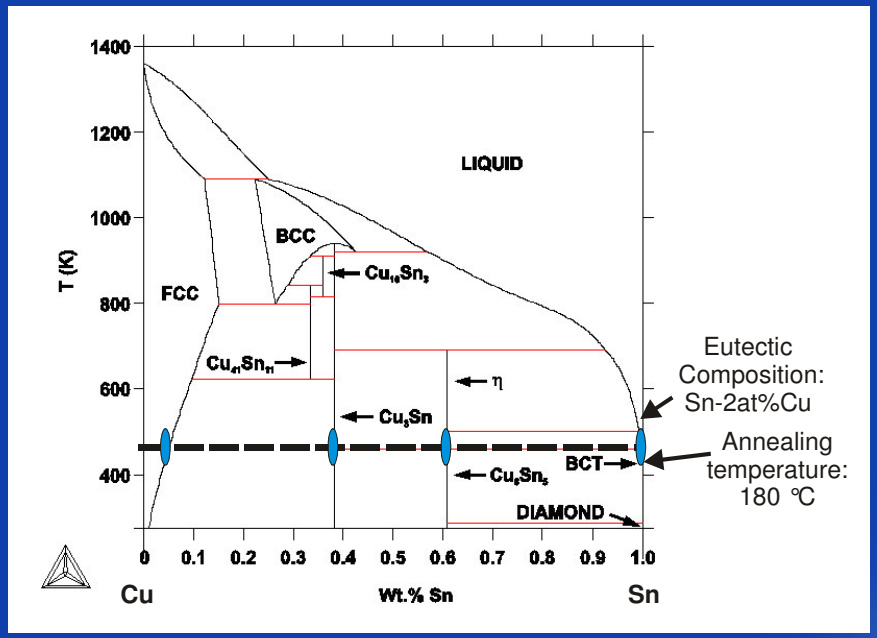

Phase field model

- **Multiple order parameter model:**

$$\eta_{(Cu),1}, \eta_{(Cu),2}, \ldots, \eta_{(Cu),i}(\vec{r},t), \ldots,$$

  - **Grains and phases**

$$\eta_{Cu_3Sn,1}, \eta_{Cu_3Sn,2}, \ldots$$

$$\eta_{Cu_6Sn_5,1}, \eta_{Cu_6Sn_5,2}, \ldots$$

$$\eta_{(Sn),1}, \eta_{(Sn),2}, \ldots \eta_{(Sn)i}, \ldots$$

    – **with** $(\eta_{(Cu),1}, \eta_{(Cu),2}, \ldots, \eta_{\rho,i}, \ldots) =$

$$(1,0,\ldots,0,\ldots),(0,1,\ldots,0,\ldots),\ldots(0,0,\ldots,1,\ldots),\ldots$$

- **Composition field:** $x_{Sn}(\vec{r},t)$

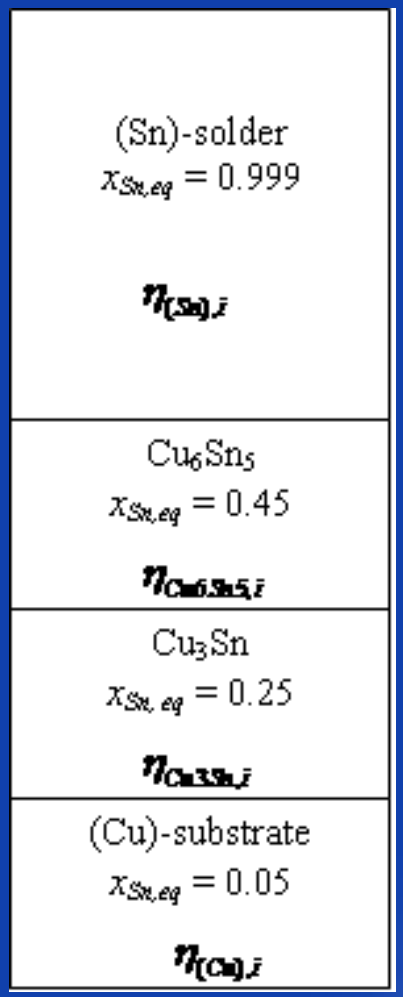

CALPHAD Gibbs energies

- COST 531-v3-0 database (+ parabolic extensions)

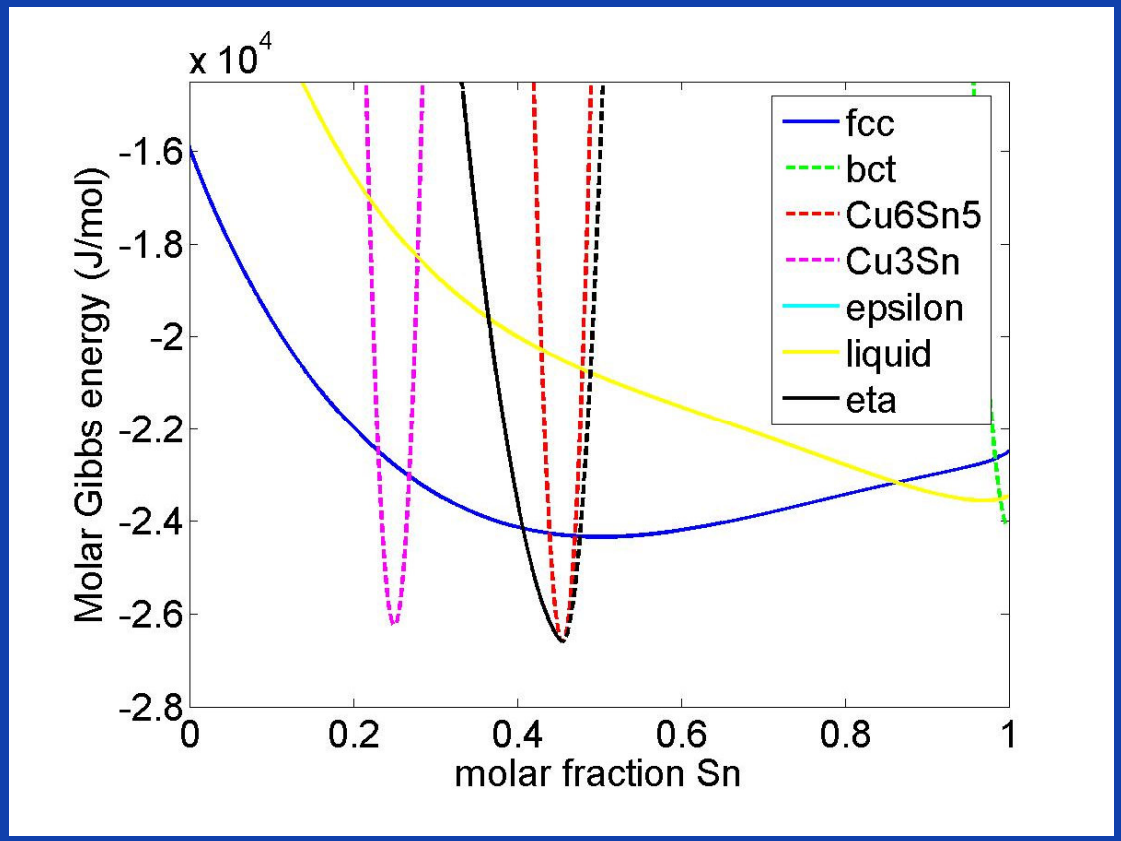

Cu-Sn

T=180 °C

A. Dinsdale, et al. COST 531-Lead Free Solders: Atlas of Phase Diagrams for Lead-Free Soldering, vols. 1,2 (2008) ESC-Cost office

IMC-layer growth (1D)

- **Effect bulk diffusion coefficient**

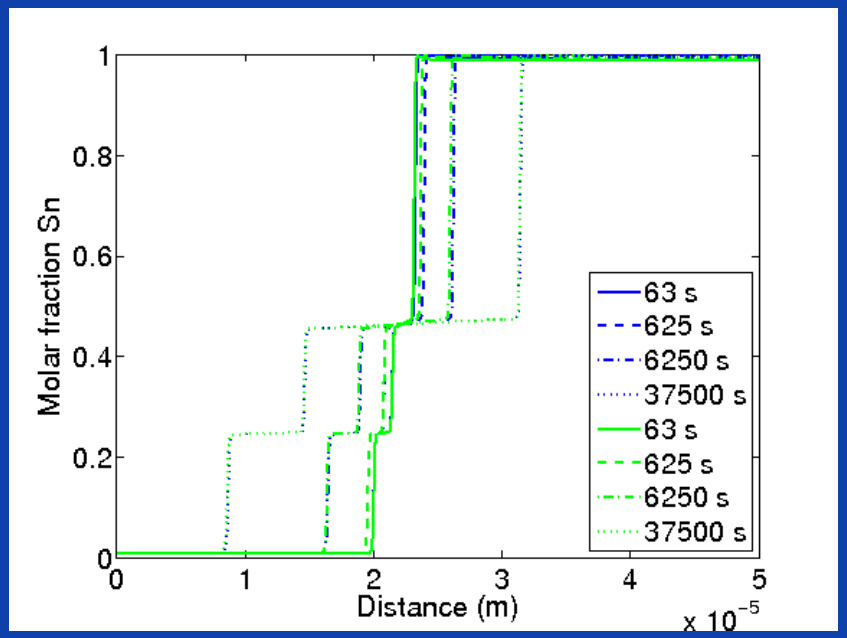

$D_{Sn}^{(Sn)} = 10^{-12}\,\mathrm{m}^2/\mathrm{s}$

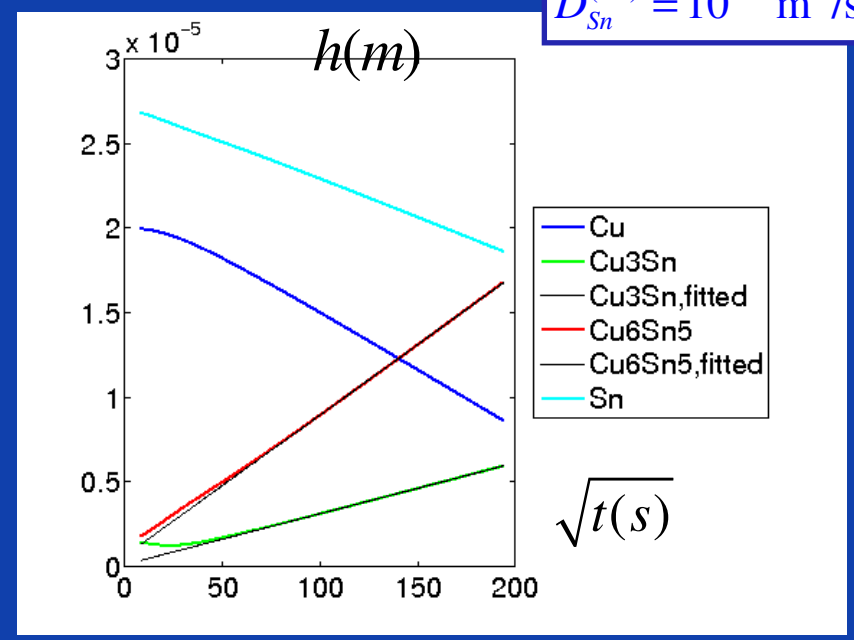

$$D_{Sn}^{(Cu)} = 10^{-25}\,\mathrm{m}^2/\mathrm{s}$$
$$D_{Sn}^{Cu3Sn} = 10^{-13}\,\mathrm{m}^2/s$$
$$D_{Sn}^{Cu6Sn5} = 10^{-13}\,\mathrm{m}^2/\mathrm{s}$$
$$D_{Sn}^{(Sn)} = 10^{-12}\,\mathrm{m}^2/\mathrm{s}$$

$$D_{Sn}^{(Cu)} = 10^{-25}\,\mathrm{m}^2/\mathrm{s}$$
$$D_{Sn}^{Cu3Sn} = 10^{-13}\,\mathrm{m}^2/s$$
$$D_{Sn}^{Cu6Sn5} = 10^{-13}\,\mathrm{m}^2/\mathrm{s}$$
$$D_{Sn}^{(Sn)} = 10^{-14}\,\mathrm{m}^2/\mathrm{s}$$

$$\Rightarrow \quad k_{Cu3Sn} = 0.0301 \cdot 10^{-6}$$
$$k_{Cu6Sn5} = 0.0833 \cdot 10^{-6}$$

$$\Rightarrow \quad k_{Cu3Sn} = 0.0306 \cdot 10^{-6}$$
$$k_{Cu6Sn5} = 0.0849 \cdot 10^{-6}$$

Comparison with experimental data

Cu3Sn, T = 180 °C

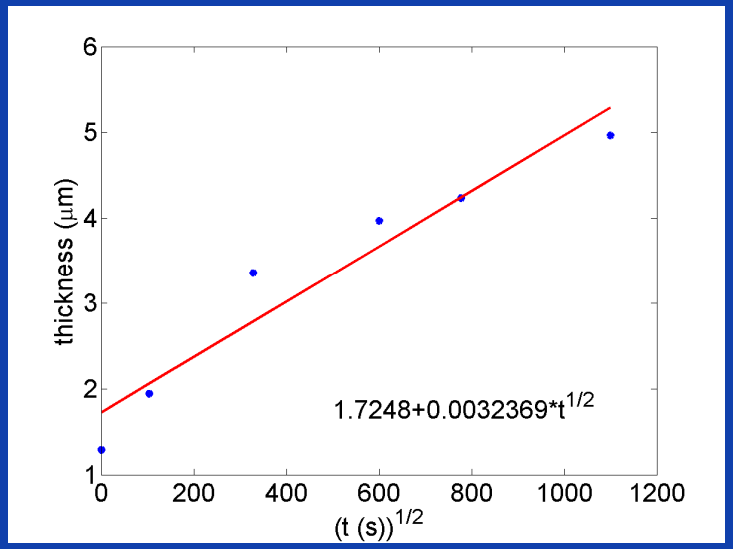

Cu6Sn5, T = 180 °C

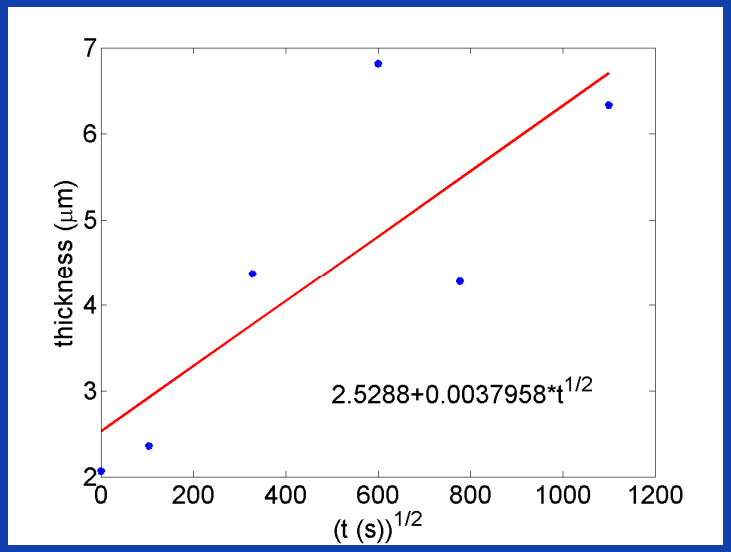

Parabolic growth constant experiments

T	k_Cu3Sn	k_Cu6Sn5
150 °C	0.0010 10^{-6}	0.00032 10^{-6}
180 °C	0.0032 10^{-6}	0.0038 10^{-6}
200 °C	0.0043 10^{-6}	0.0071 10^{-6}

Parabolic growth constant in simulations with

$$D_{Sn}^{(Cu)} = 10^{-25}\,\mathrm{m}^2/\mathrm{s}$$
$$D_{Sn}^{Cu3Sn} = 10^{-15}\,\mathrm{m}^2/\mathrm{s}$$
$$D_{Sn}^{Cu6Sn5} = 10^{-15}\,\mathrm{m}^2/\mathrm{s}$$
$$D_{Sn}^{(Sn)} = 10^{-12}\,\mathrm{m}^2/\mathrm{s}$$

$$\Rightarrow \quad k_{Cu3Sn} = 0.0023 \cdot 10^{-6}$$
$$k_{Cu6Sn5} = 0.0073 \cdot 10^{-6}$$

- **J. Janckzak, EMPA**

KATHOLIEKE UNIVERSITEIT LEUVEN

Effect of grain boundary diffusion

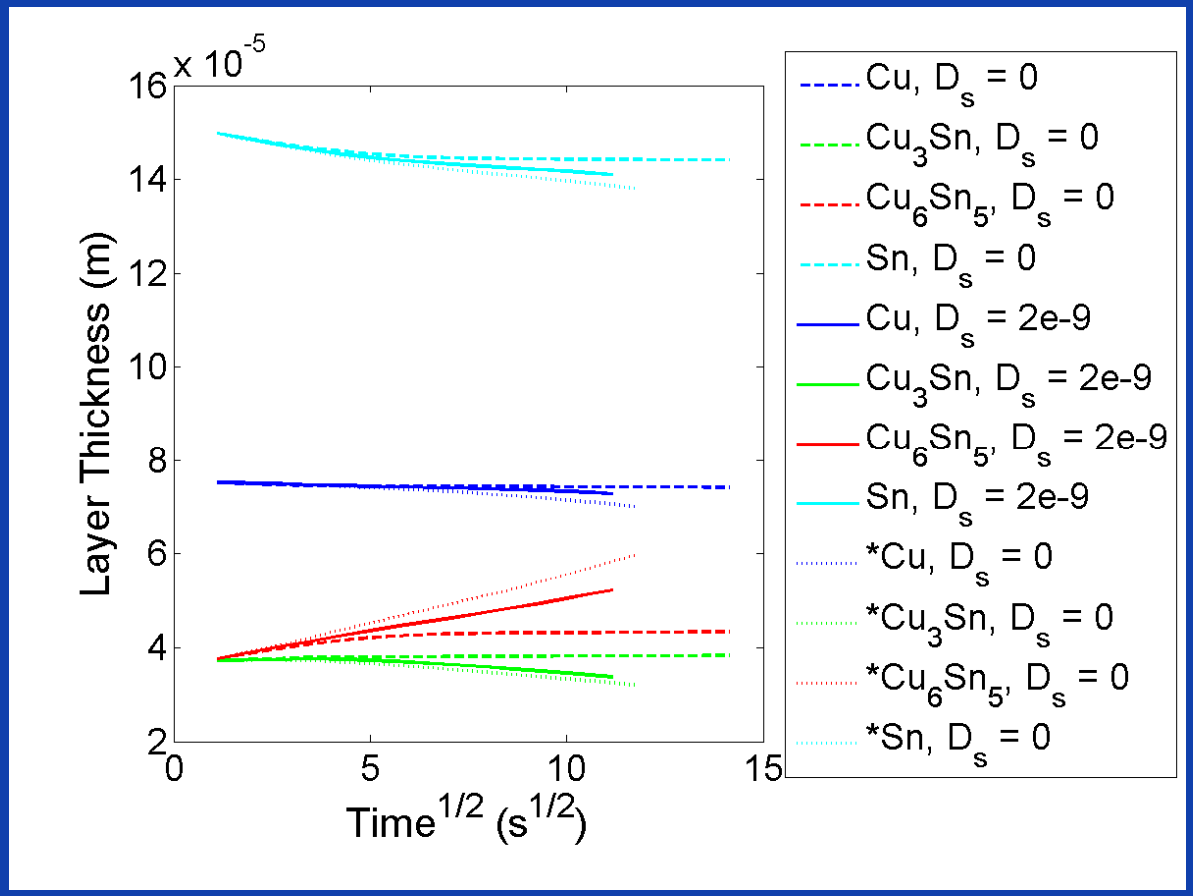

$$D_{Sn}^{(Cu)} = 2\cdot 10^{-25}, {}^{*}2\cdot 10^{-25}\,\mathrm{m^2/s}$$

$$D_{Sn}^{Cu3Sn} = 2\cdot 10^{-15}, {}^{*}2\cdot 10^{-13}\,\mathrm{m^2/s}$$

$$D_{Sn}^{Cu6Sn5} = 2\cdot 10^{-15}, {}^{*}2\cdot 10^{-13}\,\mathrm{m^2/s}$$

$$D_{Sn}^{(Sn)} = 2\cdot 10^{-12}, {}^{*}2\cdot 10^{-12}\,\mathrm{m^2/s}$$

$$\gamma_{gb} = 0.25 \quad \mathrm{J/m^2}$$

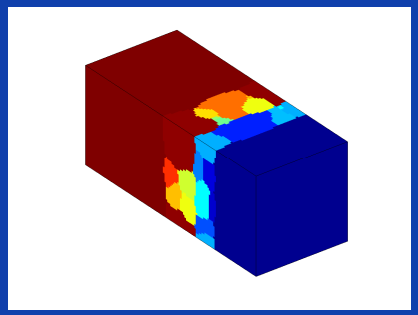

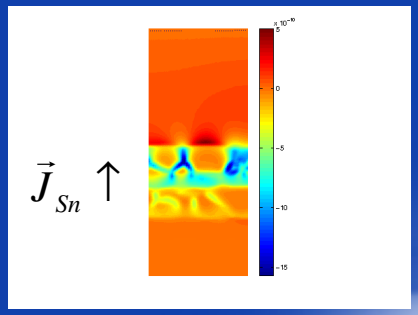

KATHOLIEKE UNIVERSITEIT LEUVEN

Growth behavior Cu_3Sn ?

Grain structure **Composition: x_{Sn}**

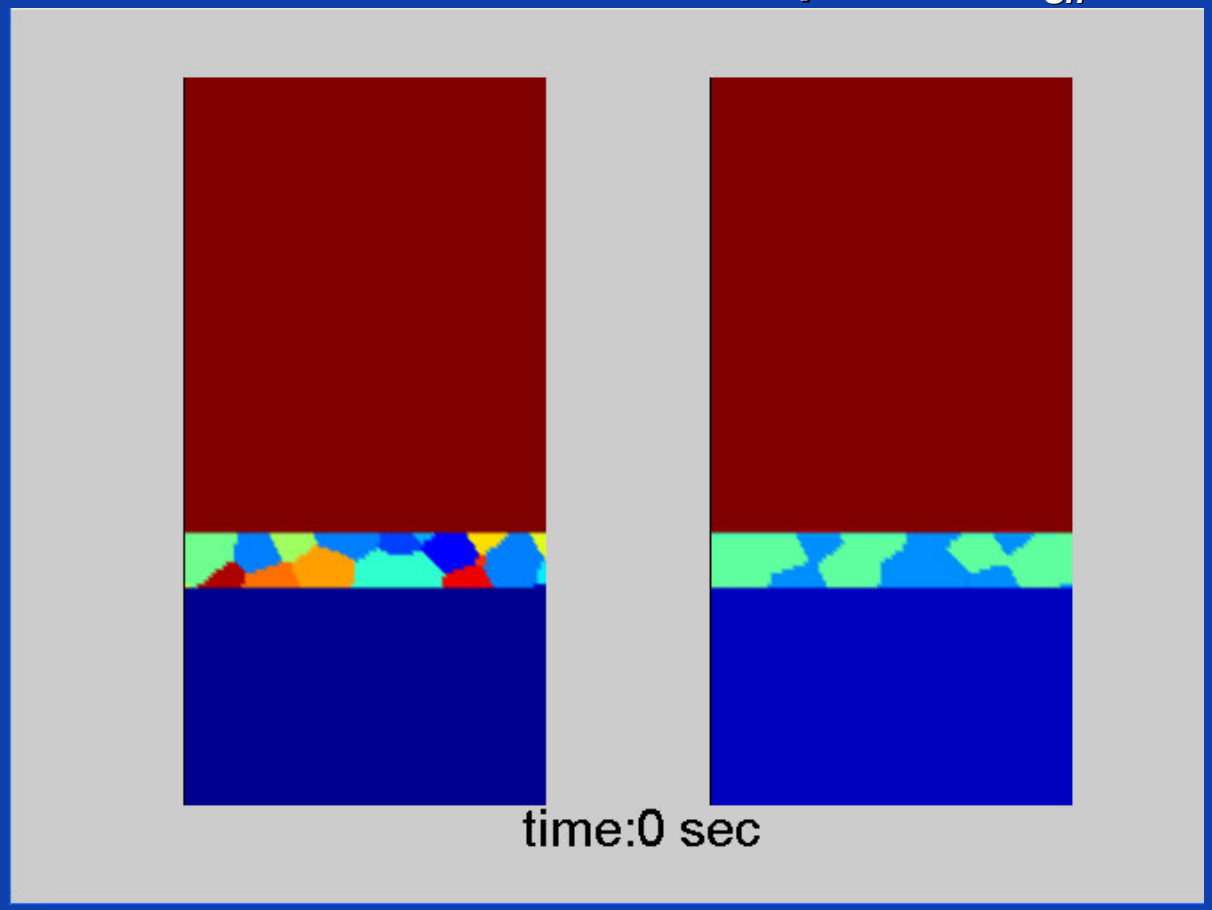

$$D_{Sn}^{(Cu)} = 2 \cdot 10^{-25}\,\mathrm{m}^2/\mathrm{s}$$

$$D_{Sn}^{Cu3Sn} = 2 \cdot 10^{-15}\,\mathrm{m}^2/\mathrm{s}$$

$$D_{Sn}^{Cu6Sn5} = 2 \cdot 10^{-15}\,\mathrm{m}^2/\mathrm{s}$$

$$D_{Sn}^{(Sn)} = 2 \cdot 10^{-12}\,\mathrm{m}^2/\mathrm{s}$$

$$\mathrm{D}_{Sn}^{surf} = 2 \cdot 10^{-12}\,\mathrm{m}^2/\mathrm{s}$$

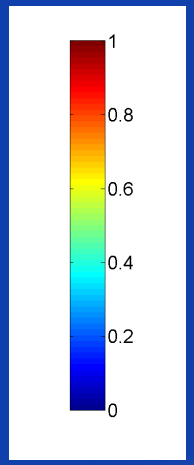

Conclusions

- What do we need next to improve the quantitative accuracy of phase-field models ?
  - Accurate representation of triple-junction angles outside [100°-140°]
  - CALPHAD Gibbs energies over full composition domain, also for stoichiometric phases and metastable regions
  - Composition and orientation dependent expressions for diffusion and interfacial properties

KATHOLIEKE UNIVERSITEIT LEUVEN

Thank you for your attention !

- **Acknowledgements**
  - **Postdoctoral fellow of the Research Foundation - Flanders (FWO-Vlaanderen)**
  - **Simulations were performed on the Flemisch Super Computer (VSC)**
  - **Projects**
    - **OT/07/040 (Quantitative phase field modelling of coarsening in lead-free solder joints)**
    - **IUAP Program DISCO (Dynamical Systems, Control, and Optimization**
    - **IWT grant SB-73163 (Phase-Field Modelling of the Solidification of Oxidic Systems)**
- **More information on *http://nele.studentenweb.org***

WORKSHOP

'Multiscale simulation of heterogeneous materials and coupling of thermodynamic models'

January 12-14, 2011

Home | Program | Registration | Venue | Sponsors | Contact

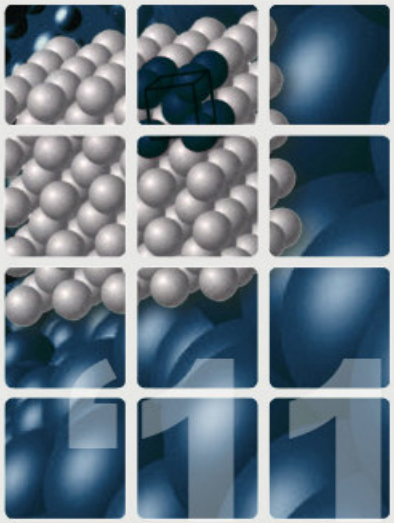

PROGRAM

Confirmed speakers:

Mathematical multiscale techniques

Serge Prudhomme (Institute for Computational Engineering and Sciences, University of Texas at Austin, USA)
Goal-oriented adaptivity for multiscale coupling methods

Mitchell Luskin (School of Mathematics, University of Minnesota, USA)
TBA

Frederic Legoll (CERMICS, ENPC, Paris, France)
TBA

Marc Geers (Mechanical Engineering, Eindhoven University of Technology, the Netherlands)
TBA

Tim Schulze (Dept. of Mathematics, University of Tennesssee, USA)
Kinetic Monte Carlo simulation of heterostructured nanocrystalline growth

Aleksander Donev (Courant Institute, New York University, USA)
Coarse-grained particle, continuum and hybrid models for complex fluids

Thermodynamic techniques/Alloys

Chris Wolverton (Dept. of Materials Science and Engineering, Northwestern University, USA)
TBA

Xavier Gonze (Physical Chemistry and Physics of Materials, Université Catholique de Louvain, Belgium)
TBA

Carolyne Campbell (NIST/Metallurgy Division, USA)
Development of Multicomponent Diffusion Mobility Databases for Industrial Processing

Webpage:

http://www.cs.kuleuven.be/conference/multiscale11/

This meeting is supported by IMACS

Copyright 2010 © Katholieke Universiteit Leuven

KATHOLIEKE UNIVERSITEIT LEUVEN

thermo search group

Multi-grain and multi-phase models

- **Multi-phase-field model**
  - **Phase fields** $\varphi_1, \varphi_2, \varphi_3, \ldots \varphi_p, \quad \sum_{i=1}^{p} \varphi_i = 1$
  - **Free energy** $$f_{\text{int}} = \sum_{i \neq j} \frac{4\sigma_{i,j}}{\eta_{i,j}} \left\{ \frac{\eta_{i,j}^2}{\pi^2} |\nabla \phi_i \cdot \nabla \phi_j| + \phi_i \phi_j \right\}$$ $$0 < \phi_{i,j} < 1$$
    - **Double obstacle, higher order terms, gradient term non-variational**
    - **Interpolation: zero-slope or thermodynamic consistency**

Steinbach et al.

MICRESS phase-field code

H. Garcke, B.Nestler, B. Stoth, SIAM J. Appl. Math. 60 (1999) p 295.

L.-Q. Chen and W. Yang, PRB, 50 (1994) p15752

- **Multi-order parameter models**
  - **Order parameters** $\eta_1, \eta_2, \ldots, \eta_i(\vec{r}, t), \ldots, \eta_p, \quad \left(\sum_{i=1}^{p} \eta_i \neq 1 \right)$
  - **Interfacial energy** $$f_{\text{int}} = m \left(\sum_{i=1}^{p} \left(\frac{\eta_i^4}{4} - \frac{\eta_i^2}{2} \right) + \sum_{i=1}^{p} \sum_{j<i}^{p} \gamma_{i,j} \eta_i^2 \eta_j^2 + \frac{1}{4} \right) + \frac{\kappa(\eta)}{2} \sum_{i=1}^{p} (\vec{\nabla} \eta_i)^2$$

A. Kazaryan et al., PRB, 61 (2000) p14275

KATHOLIEKE UNIVERSITEIT LEUVEN

Multi-grain and multi-phase models

- **Vector valued model**
  - **Orientation field (θ) and phase field (ϕ)**
  - **Free energy** $f_{\text{int}} = f(\phi, |\nabla\phi|, |\nabla\theta|)$

R. Kobayashi, J.A. Warren, W.C. Carter, Physica D, 119 (1998) p415

- **2-phase solidification**
  - **Phase fields** $\varphi_1, \varphi_2, \varphi_3, \quad \sum_{i=1}^{3} \varphi_i = 1$
  - **Fifth order interpolation functions $g_i(\phi_1, \phi_2, \phi_3)$**
    - **Zero-slope and thermodynamic consistent**
    - ***Order g_i* increases with number of phase-fields**

R. Folch and M. Plapp, PRE, 72 (2005) n° 011602

- **Multi-order parameter + 4th order gradient terms**

I.M. McKenna, M.P. Gururajan, P.W. Voorhees, J. Mater. Sci., 44 (2009) p2206

- **Phase field crystal and amplitude equations**

Bounding Box Algorithm

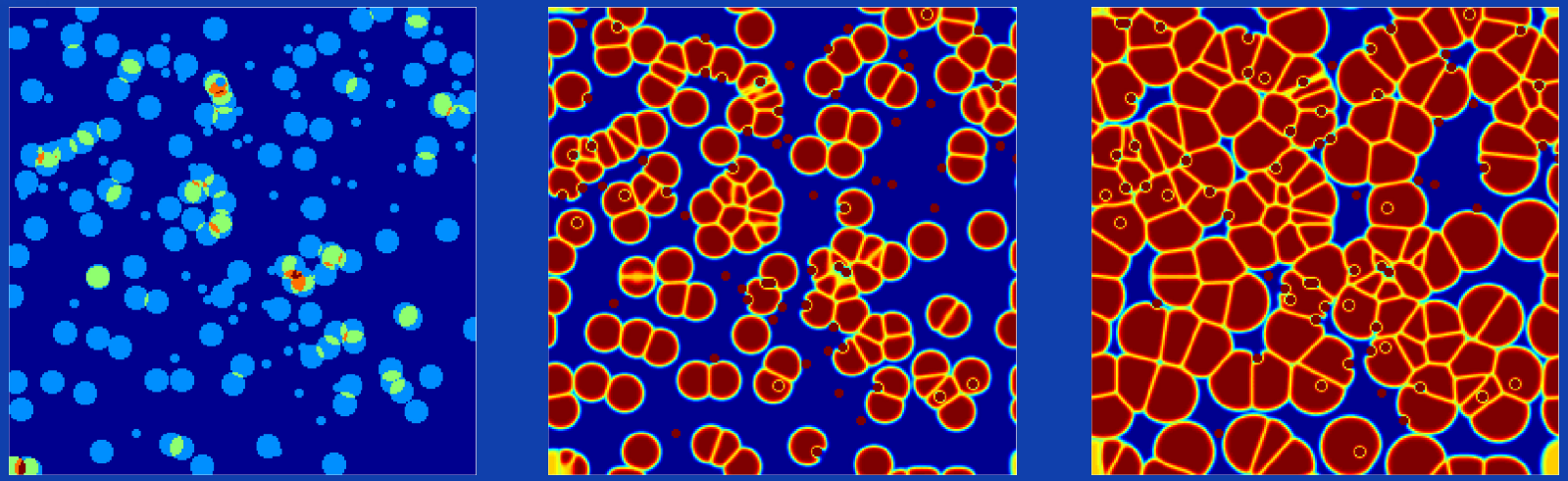

- Initialization by random nucleation
  - Generate sphere-shaped grain uniformly over microstructure
  - Generate particles uniformly over microstructure
- Set-up sparse data structure
  - Determine bounding box for every grain
  - Create object for every grain